Desalination and Water Treatment
www.deswater.com
doi: 10.1080/19443994.2014.927125

53 (2015) 2388–2402
March

Taylor & Francis
Taylor & Francis Group

Characteristics of the adsorbed heavy metals onto aerobic granules: isotherms and distributions

Ki Hong Ahn[a], Seok Won Hong[b,*]

[a]*Phillips Exeter Academy, 20 Main Street, Exeter, NH 03833, USA*
[b]*Center for Water Resource Cycle Research, Korea Institute of Science and Technology, Hwarangno 14-gil 5, Seongbuk-gu, Seoul 136-791, Republic of Korea, Tel. +82 2 958 5844; Fax: +82 2 958 5839; email: swhong@kist.re.kr*

Received 15 April 2013; Accepted 13 May 2013

ABSTRACT

Biosorption experiments were performed using aerobic granules as bioadsorbent for Cd^{2+}, Cu^{2+}, Mn^{2+}, Zn^{2+}, Fe^{2+}, and Co^{2+}. Aerobic granule shows high adsorption capacity [Q_e (mg/g) = 189 − 232]. Both Langmuir and Freundlich isotherm fitted the adsorption data well. Especially, the R^2 value exceeds 0.96 in most cases when Langmuir model was adopted. In order to look into the distribution of the adsorbed heavy metal in aerobic granules and to verify metal uptake in surface layer, in middle zone and center of aerobic granule, energy dispersive X-ray (EDX) spectra were obtained. According to field emission scanning electron microscope-EDX observation, it was found that whole granule body can act as an active site for heavy metals uptake because of a lot of pore existed in the inside of aerobic granule. It is clear that the penetration of dissolved metal solution to the center of aerobic granule has occurred, which confirms that metal uptake can occur even in the center of aerobic granule. The analyses by Fourier transform infrared spectroscopy and X-ray photoelectron spectroscopy showed that functional groups on aerobic granules, such as alcoholic, carboxylate and ether, would be the main binding sites for biosorption of heavy metals. The area distributions further reveal that ether and alcoholic would be the dominant carbon forms in aerobic granules, and the interaction and coordination affinity between the functional groups and metals would be more complicated than expected.

Keywords: Aerobic granules; Heavy metal biosorption; Adsorption isotherms; FESEM-EDX analysis; FTIR analysis; XPS analysis

1. Introduction

The disposal of wastewater containing heavy metals is related to various industrial activities, such as: electroplating, chemical manufacture, leather tanning, oil refining, and especially mining and mineral processing [1]. These industrial activities have intensified environmental pollution with the accumulation of heavy metals [2,3]. Commonly used physiochemical methods for removal of heavy metals from aqueous solutions include precipitation, ion exchange, electrochemical processes, and membrane processes such as nanofiltration and reverse osmosis [4]. However, conventional methods of metal removal from wastewater are expensive in terms of energy consumption and not always effective for metals in low concentrations [5].

*Corresponding author.

Biosorption of heavy metals from aqueous solution have emerged as an eco-friendly, efficient, and cost-effective method [6]. Studies using biosorbents, e.g. agricultural wastes, fungi, algae, seaweed, and bacteria have shown that both living and dead microbial cells are able to adsorb metal ions and offer potential inexpensive alternative to conventional adsorbents [7–15]. Mostly, biosorbents are used in the forms of bioflocs and suspended aggregates of micro-organisms. One of the major operational problems associated with suspended flocs is that a post-separation of biosorbent from the treated effluent is required [16]. To overcome this drawback, in process applications, upflow sludge columns, batch and membrane rector systems, activated sludge-biofilm process, granular activated carbon-sequencing batch reactor (SBR) system, biomass immobilized system, and fixed-bed column with anaerobic biomass are commonly proposed to retain biomass cells in the reactor system, thus enhancing the operation performance for heavy metal removal through biosorption [17–23]. Meanwhile, intensive research has been conducted to understand the mechanism of aerobic granulation in a SBR and its application in treating a wide variety of municipal and industrial wastewater [24]. Recent studies have demonstrated that aerobic granules having compact, porous structure, and excellent settling ability can be cultivated in SBR [16,24–26]. Such characteristics suggest that aerobic granules would be a valuable candidate as biosorbents for heavy metal removal from wastewater [16]. A few attempts have been made to study the biosorption characteristics of the aerobic granules [16,27–31] using model heavy metals such Cd, Cu, Ni, Cr, and Be, in terms of kinetic model, thermodynamics, and biosorption mechanisms. These studies indicated that ion exchange would be the main mechanism involved in biosorption of Cd, Cu, and Ni, while metal complexation, chemical precipitation, and ion exchange were mainly involved in the removal of Cr, and the functional groups like carboxyl and hydroxyl played an important role in the biosorption of Be, respectively. But there is no information about the effect of aerobic granules porosity except Yu and Hui [32]. Following to the Yu and Hui using Ni as a model heavy metal, the energy dispersive X-ray (EDX) analysis indicated that Ni^{2+} ion could penetrate into the core of aerobic granule, and the distribution of the adsorbed Ni^{2+} in the aerobic granule seemed uniform. If these phenomena could have occurred commonly in aerobic granules for sorption of heavy metals, aerobic granules could be competitive and excellent biomaterials for the removal of heavy metals because whole body of aerobic granule can be used as an active site for biosorption. We, therefore, have investigated whether other heavy metals, i.e. Cd^{2+}, Cu^{2+}, Mn^{2+}, Zn^{2+}, Fe^{2+}, and Co^{2+}, can penetrate well into the core of aerobic granules and how they are distributed in the aerobic granules in terms of isotherm models such as the simple Langmuir and Freundlich equations, and field emission scanning electron microscope-energy dispersive X-ray spectroscopy (FESEM-EDX) analysis and Fourier transform infrared spectroscopy (FTIR) and X-ray photoelectron spectroscopy (XPS) analysis.

2. Materials and methods

2.1. Aerobic granules and preparation of heavy metal ion solution for biosorption

The aerobic granules used in this study were cultivated in a SBR with a working volume of 5L. The SBR was operated in a time sequence of 5 min feeding, 240 min of aeration, 5 min settling, and 1 min of effluent withdrawal. The treated wastewater was discharged from the middle port of the SBR reactor. Synthetic wastewater used in this study was mainly composed of sodium acetate as sole carbon source, while its detail compositions can be found elsewhere [33]. Mature granules were nearly spherical in shape and had a compact and integrated structure. Mature aerobic granules were freeze-dried for biosorption tests.

Heavy metal ion solutions were obtained by diluting 1.0 g/l of stock heavy metal ion solutions which was prepared by dissolving $MnCl_2{\cdot}4H_2O$, $CuCl_2{\cdot}2H_2O$, $CoCl_2{\cdot}6H_2O$, $CdCl_2{\cdot}2.5H_2O$, $ZnSO_4{\cdot}7H_2O$, $FeCl_2$ into de-ionized water, respectively. In this study, the initial heavy metal ion concentration was varied from 20 to 500 mg/l, and the initial pH of each solution was in the range of 5.5–6.2, except Fe^{2+} solution (pH value was 2.4–3.4). pH played a major role in the biosorption and possibly affected the activity of the functional groups of aerobic granules [34]. The experimental results of maximum biosorption capacity of heavy metals, by aerobic granules, at different initial pH values implied that the biosorption of heavy metals would be pH-dependent, i.e. with the increase of pH, the amount of heavy metal uptake by granules tended to increase and a sharp increase of Q_{max} (maximum metal uptake) was observed in between pH 3 and 6. At about pH 6 a plateau was reached, e.g. there was no significant difference between the maximum heavy metal biosorption capacity at pH 6 and 7 [27,29]. In this study, initial pH was kept at 6.0 ± 0.2 for model heavy metals, except Fe^{2+} solution. For the case of Fe^{2+}, pH was adjusted to 3.0 ± 0.2 because precipitation occurred as pH increased.

2.2. Batch biosorption experiments

In batch test, each 1 g of freeze-dried aerobic granules were placed in Jar-tester bottle (1,000 ml) to directly contact with 500 ml of metal-bearing solutions (Cd^{2+}, Cu^{2+}, Mn^{2+}, Zn^{2+}, Fe^{2+}, and Co^{2+}), already fixed at pH mentioned above, of 500, 350, 200, 100, 50, and 20 mg/l of initial metal concentrations, to determine heavy-metal removal capacity of aerobic granules, respectively. All the experiments were conducted at 20˚C. The metal bearing solutions in which aerobic granules were placed were agitated on a Jar-tester at 150 rpm for 2 h, which is sufficient to reach sorption equilibrium of each heavy metal (data not shown). After 2 h, aerobic granules were removed from the solution and freeze-dried again for the analysis of heavy metal adsorbed on aerobic granules, and the supernatant fraction was taken using a syringe. The supernatant filtered with 0.45 μm of membrane filter was analyzed for the soluble heavy metal concentration. Soluble Cd^{2+}, Cu^{2+}, Mn^{2+}, Zn^{2+}, Fe^{2+}, and Co^{2+} concentrations in solution were analyzed by ICP-AES (Prodigy, Leeman Labs Inc.).

2.3. FESEM-EDX, FT-IR, and XPS analysis

The surface morphologies and elemental compositions of aerobic granules before and after heavy metal biosorption were examined by field emission scanning electron microscope (FESEM, Hitachi S-4100) coupled with EDX (Horiba EMAX 6853-H). The freeze-dried granule samples were mixed with spectroscopic quality KBr in the ratio of 1:100 for the measurement of FT-IR (Perkin Elmer Spotlight 200 microscope system) spectroscopy to identify and evaluate the functional groups that can be involved in the sorption process. FT-IR spectra of aerobic granules before and after adsorption were recorded in the range of 500–4,000 cm^{-1}. The background absorbance was measured using pure KBr pellets. XPS measurement was performed for more insights into the mechanisms of biosorption of aerobic granules. XPS spectra were recorded on a PHI 5000 VersaProbe (ULVAC-PHI) using a monochromated Al Kα X-ray source (1486.6 eV of photons) operated at 15 kV and 25 W. For calibration, the binding energy (BE) of the spectra was standardized with the C1s peak at 284.6 eV.

2.4. Data evaluation

The amount of metal ion adsorbed by aerobic granules was calculated using the mass balance equation:

$$Q_e M = V(C_o - C_e) \quad (1)$$

where Q_e is the loading capacity of the adsorbent (mg adsorbate/g adsorbent); V is the solution volume in the vessel (l); C_o, C_e are the initial and final concentration of the metal ion, respectively (mg/l); and M is dry mass of the adsorbent (g).

Two of the most common sorption models were used to fit the experimental data. The Langmuir model which assumes that equilibrium is attained when a monolayer of the adsorbate molecules saturates the adsorbent [14,27]. This mode can be written as:

$$Q_e = Q_{max} b C_e / (1 + b C_e) \quad (2)$$

where Q_{max} is the maximum metal uptake under the given conditions; b is a constant related to the affinity between the adsorbent and the adsorbate [14,34]. The linear form of Langmuir model is:

$$1/Q_e = 1/Q_{max}(1/bC_e + 1) \quad (3)$$

The second model is Freundlich model which can be written as:

$$Q_e = kC_e^{(1/n)} \quad (4)$$

where k and n are Freundlich constants, which are correlated to the maximum adsorption capacity and adsorption intensity, respectively [14]. The linear form of this model takes the form:

$$\log Q_e = \log k + 1/n \log C_e \quad (5)$$

3. Results and discussion

3.1. Adsorption isotherms

The mean size of the granules was about 1.0 mm. It can be seen that a considerably different pore size distribution (maximum 300 μm) existed inside the aerobic granules. The sphere type of particle observed in aerobic granules was identified as a calcium lump which fed to the reactor for producing aerobic granules (Fig. 1).

Fig. 2 shows the adsorption isotherm of Cd^{2+}, Cu^{2+}, Mn^{2+}, Zn^{2+}, Fe^{2+}, and Co^{2+} ions using aerobic granules at 20˚C. The analysis of the experimental

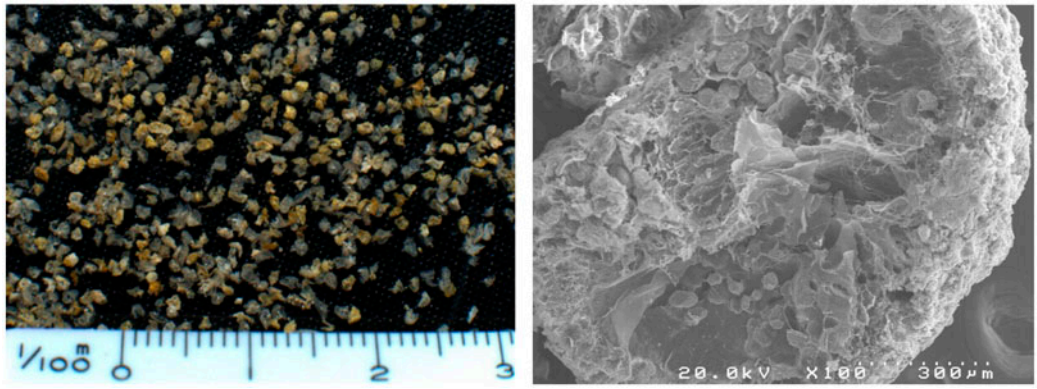

Fig. 1. Freeze-dried type of aerobic granules used in this experiment and the morphology of aerobic granules obtained using FESEM.

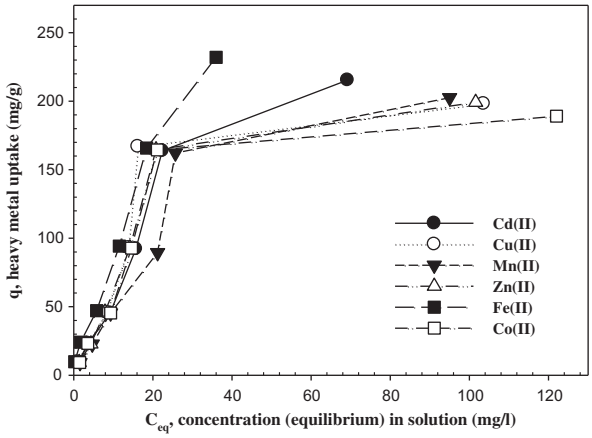

Fig. 2. Adsorption isotherm of Cd^{2+}, Cu^{2+}, Mn^{2+}, Zn^{2+}, Fe^{2+}, and Co^{2+} ions using aerobic granules at 20°C (pH 6 for Cd^{2+}, Cu^{2+}, Mn^{2+}, Zn^{2+}, and Co^{2+}; pH 3 for Fe^{2+}).

results of Cd^{2+}, Cu^{2+}, Mn^{2+}, Zn^{2+}, and Co^{2+} biosorption at the same equilibrium pH (pH 6.0) shows that adsorbent affinity follows the order: Cd(Q_e (mg/g) = 215.4) > Mn(Q_e (mg/g) = 202.5) > Zn(Q_e (mg/g) = 199) > Cu(Q_e (mg/g) = 198.2) > Co(Q_e (mg/g) = 189).

Compared with activated sludge [Q_e (mg/g) = 30–90] for Cd^{2+} and Cu^{2+} [14], aerobic granules show higher adsorption efficiency [Q_e (mg/g) = 189–215.4]. Previous research showed that the adsorption capacity of Cd^{2+} by aerobic granules was 200 mg Cd^{2+}/g dry weight of granules [16], while 215.4 mg Cd^{2+}/g weight of granules was obtained in our study. Factors like pH, concentration of metal present in the wastewater, composition, and characteristics of wastewater and sludge may influence the biosorption process [3]. Metal removal by sludge is a consequence of interaction between metals in the solution and the bacterial cell surface, and follows complex mechanisms, mainly ion exchange, chelation, and adsorption by physical forces [6]. The adsorption of heavy metals on the sludge surface is usually attributed to the formation of complexes between metals and carboxyl, hydroxyl, and phenolic surface functional groups of the extracellular polymeric substances (EPS). These biopolymers which can be produced by many different species of bacteria isolated from activated sludge have been shown to be involved in the adsorption of metal ions from solution [3,35]. EPS has been found in almost all forms of microbial aggregates, including bioflocs, biofilm, anaerobic, and aerobic granules. However, the content of EPS in aerobic granules was found to be much higher than that in conventional bioflocs and biofilms [36]. Wang et al. [37] reported that along with aerobic granulation in an SBR, both biomass and EPS concentrations tended to increase, and a decreased sludge volume index was found accordingly. For example, the EPS content in the mature aerobic granules was about 47 mg/g MLSS (mixed liquor suspended solids), whereas it was only 17 mg/g MLSS in the seed activated sludge [37]. Even if it is not clear that higher EPS content is the major factor of higher metal uptake capacity of aerobic granules than activated sludge, Liu et al. [16] seems to imply that aerobic granules would be associated with an increase in the EPS content. Meanwhile, for the case of Fe^{2+}, the highest metal uptake capacity was shown as 232 mg of Fe^{2+}/g of granules in the range of pH 2.4–3.4. Normally, at low values of pH the decrease in the removal efficiency could be referred to the fact that the mobility of the hydrogen ions is higher than that of the metal ions and it reacts with active sites before adsorbing the metal ions [14]. At low pH value, cell wall functional groups are closely associated with hydrogen ion and restricted the approach of metal

cations as a result of the repulsive force [38,39]. As the pH increases, more functional groups on the cell surface would be exposed, and result in an increase of negative charges with sequent attraction of metallic ions with positive charge. According to Xu et al. [27], at pH 2, the aerobic granules have a positive charge associated with an extremely low biosorption capacity for the Ni^{2+}. However, at pH 3–5, the amount of Ni^{2+} removed by aerobic granules increased sharply due to the steep decrease of the zeta potential of aerobic granules. There is no significant change in the Ni^{2+} biosorption capacity of aerobic granules. In our result, the highest metal uptake capacity for Fe^{2+} in the range of pH 2.4–3.4 might indicate that, possibly, factors other than electrostatic attraction are involved in the mechanism of Fe^{2+} biosorption by aerobic granules.

3.2. Adsorption isotherm models

Many sorption isotherm models are usually used to fit the adsorption isotherm data in order to obtain a

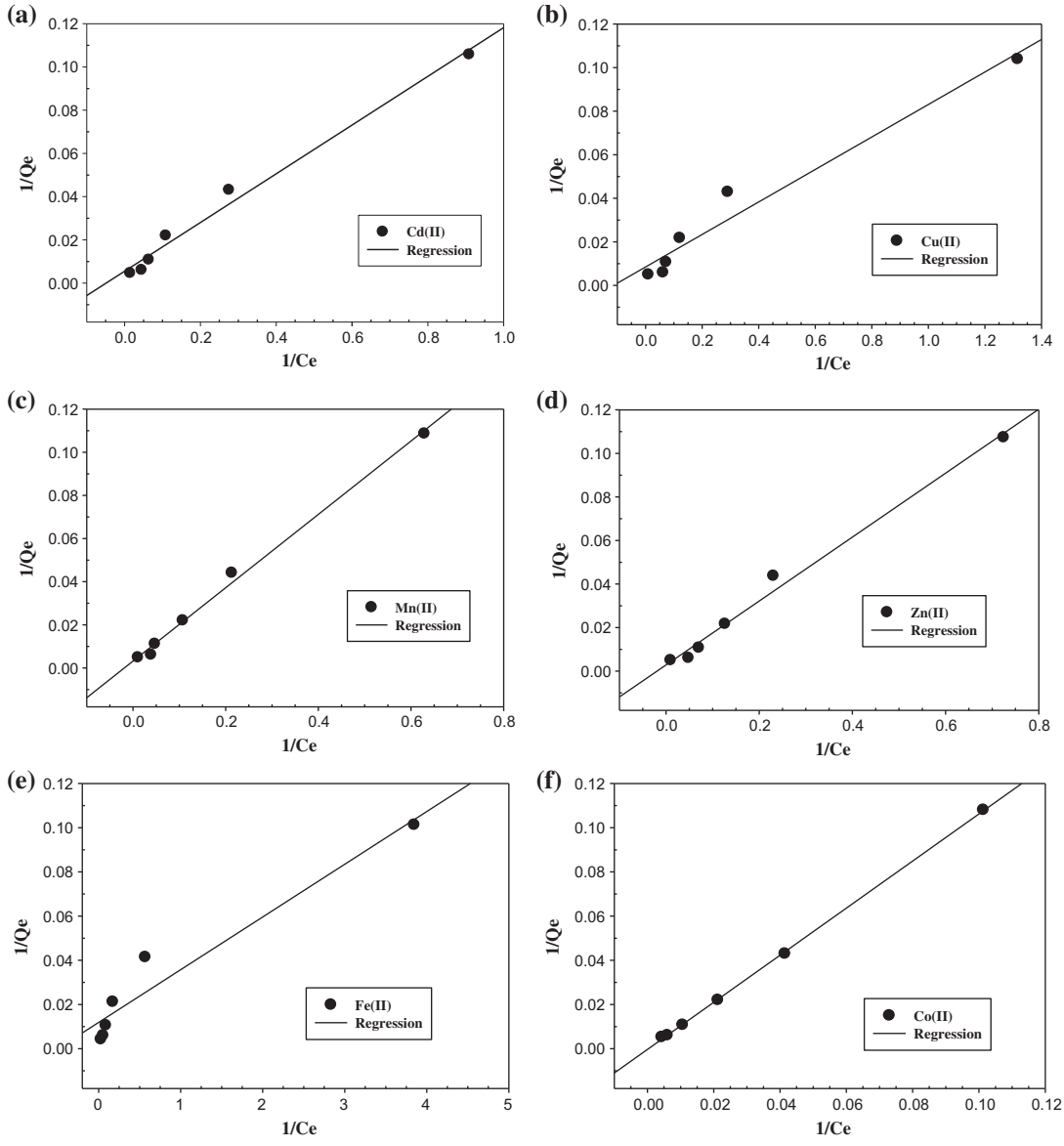

Fig. 3. Langmuir isotherms for the bioadsorption of Cd^{2+}, Cu^{2+}, Mn^{2+}, Zn^{2+}, Fe^{2+}, and Co^{2+} by aerobic granules at 20°C, pH 6 for Cd^{2+}, Cu^{2+}, Mn^{2+}, Zn^{2+}, and Co^{2+}; pH 3 for Fe^{2+} (a: Cd^{2+}, b: Cu^{2+}, c: Mn^{2+}, d: Zn^{2+}, e: Fe^{2+}, and f: Co^{2+}).

linear regression data to predict the maximum adsorption capacity of the adsorbent. Langmuir and Freundlich models are the most widely used models in the case of the adsorption of metal ions with bioadsorbents even though the metal uptake may not exactly follow the monolayer adsorption mechanism assumed in the former model [14].

Fig. 3 shows plots of Langmuir isotherms for the biosorption of Cd^{2+}, Cu^{2+}, Mn^{2+}, Zn^{2+}, Fe^{2+}, and Co^{2+} by aerobic granules, respectively. The linear plots of $1/Q_e$ against $1/C_e$ show that the adsorption of six different heavy metals ions by aerobic granules fits very well to Langmuir model.

The same data is plotted using Freundlich models as shown in Fig. 4. Compared to the Langmuir model, the metal ions adsorption by the aerobic granules does not obey well with the Freundlich model, except for Fe^{2+} ions. For the case of Fe^{2+} ions, the adsorption of Fe^{2+} ions by aerobic granules fits very well to Freundlich model.

The two model constants for six different ions in addition to R^2 values for each line are summarized in

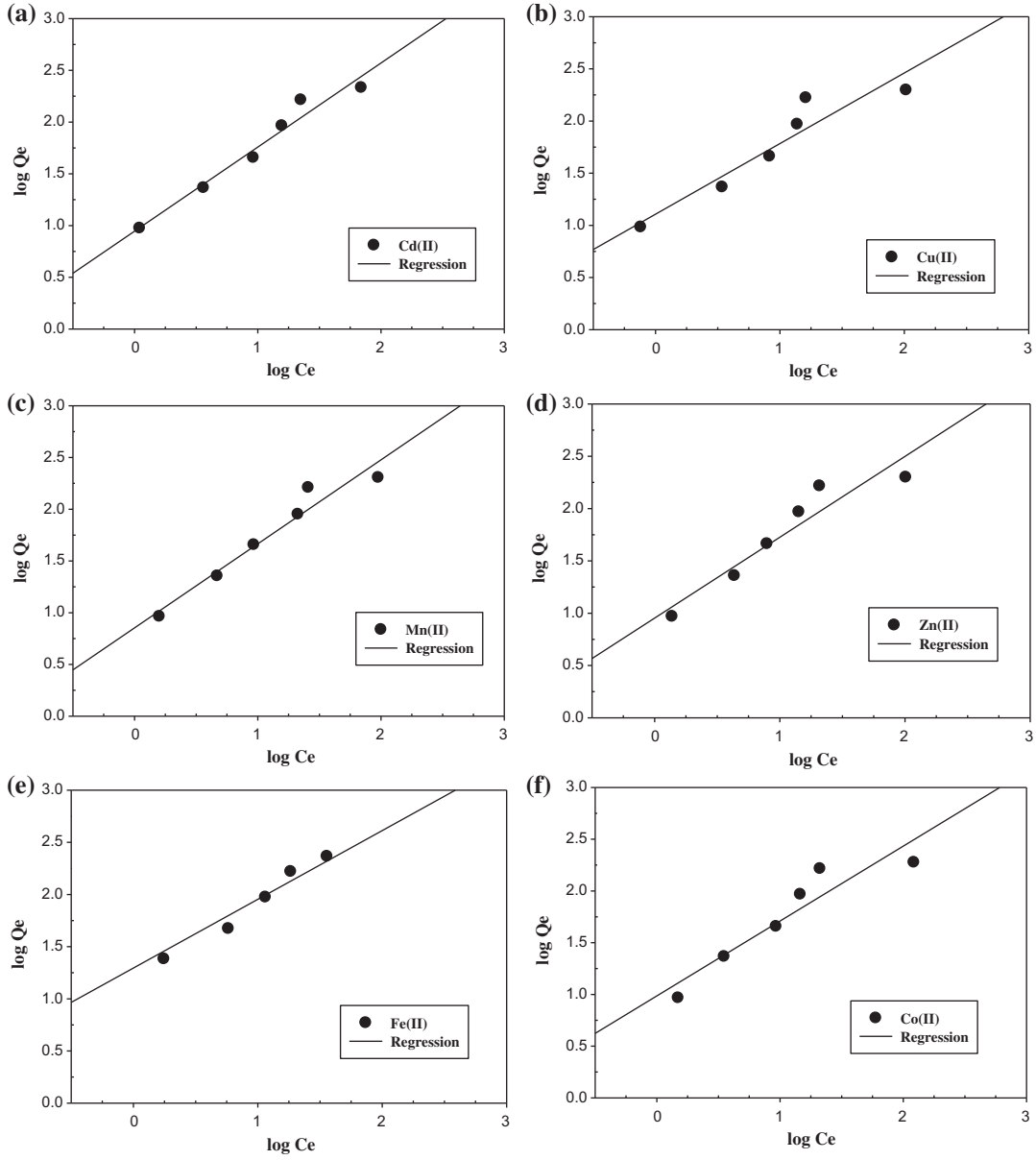

Fig. 4. Freundlich isotherms for the bioadsorption of Cd^{2+}, Cu^{2+}, Mn^{2+}, Zn^{2+}, Fe^{2+}, and Co^{2+} by aerobic granules at 20°C, pH 6 for Cd^{2+}, Cu^{2+}, Mn^{2+}, Zn^{2+}, and Co^{2+}; pH 3 for Fe^{2+} (a: Cd^{2+}, b: Cu^{2+}, c: Mn^{2+}, d: Zn^{2+}, e: Fe^{2+}, and f: Co^{2+}).

Table 1
Linear regression data for Langmuir and Freundlich isotherms for the bioadsorption of the heavy metal ions with aerobic granular sludge

Ion	Langmuir parameters			Freundlich parameters		
	Q_{max}	b(×100)	R^2	k	n	R^2
Cd^{2+}	181.72	4.88	0.9873	8.81	1.23	0.9635
Cu^{2+}	117.83	113.79	0.9632	12.79	1.48	0.8907
Mn^{2+}	311.14	1.89	0.9952	17.04	1.23	0.9452
Zn^{2+}	349.65	1.95	0.9903	8.98	1.29	0.9000
Fe^{2+}	83.89	50	0.9392	19.72	1.52	0.9713
Co^{2+}	701.26	0.91	0.9948	9.68	1.38	0.8756

Table 1. In the Langmuir model, Q_{max} of Co^{2+} is 701.26 mg/g and Q_{max} of Cu^{2+} is 117.83 mg/g by aerobic granules, respectively. On the other hand, b value of Co^{2+} with aerobic granules is lower than that of Cu^{2+} and their values are 0.91 and 113.79, respectively. As the constant b is a function of the affinity of the adsorbent to the adsorbate, this means that as the b value increase the affinity increases [14]. The affinity of the adsorbent for the six different ions is in the order as follows: $Cu^{2+} > Fe^{2+} > Cd^{2+} > Zn^{2+} > Mn^{2+} > Co^{2+}$. Meanwhile, in the Freundlich model, the maximum adsorption capacity of Cu^{2+} ($k = 12.79$) is higher than that of Co^{2+} ($k = 9.68$) and adsorption intensity of Cu^{2+} ($n = 1.48$) is also higher than that of Co^{2+} ($n = 1.38$), respectively. In the Freundlich model, the affinity of the adsorbent for the six different ions is in the order as follows: $Fe^{2+} > Cu^{2+} > Co^{2+} > Zn^{2+} > Mn^{2+} = Cd^{2+}$.

3.3. Distribution of the adsorbed heavy metals in aerobic granules

Even if the adsorption of metal ions with aerobic granules follow the monolayer adsorption mechanism assumed in Langmuir model, it is necessary to explain the phenomena that metal adsorption for Co^{2+} estimated having low affinity in model show high metal uptake value [Q_e(mg/g) = 189] and unrealistically high value of Q_{max} (701.26 mg/g) in the Langmuir model, respectively. As the aerobic granule has pores within the sludge body, it is assumed that metal adsorption by aerobic granule can occur inside the aerobic granule. During the experiment, it is observed that the color change of aerobic granule has occurred within whole granule body as the metal uptake is taking place. To analyze metal adsorption within whole body of aerobic granules, EDX spectra were obtained using FESEM. For this analysis, the aerobic granules were roughly crushed to expose the interior surface. For the fresh granule, C, O, and Ca constituted the three major elements of the aerobic granule and Mg, Cl, S, and Si were detected as minor elements (data not shown). This result was consistent with a previous report showing that C, O, and Ca constituted the three major elements of the aerobic granule [32].

As shown in Fig. 5(a), aerobic granule has a large number of pores, so the metal-dissolved solution penetrates well through the pore into the center of aerobic granule and result in whole body of aerobic granule acting as an active site for metal uptake. In order to look into the distribution of the adsorbed heavy metal in aerobic granules and to verify metal uptake in surface layer, in middle zone, and center of aerobic granule, EDX spectra were obtained. As shown in Fig. 5(a), number 2, 3, 4, and 5 spots were checked for the aerobic granule used for Cu^{2+} adsorption, respectively. As shown in Fig. 5(b)–(e), sphere type of particle in number 2 spot is mainly constituted of calcium lump already mentioned above. Compared to weight % of Cu element observed in number 3 (6.06%), 4 (30.34%), and 5 (29.16%) spots, it indicates that Cu^{2+} ion uptake has occurred even in the middle zone and in the center of aerobic granule.

As shown in Fig. 6(a)–(c), EDX spectra were obtained in surface layer (no. 16 spot), in middle zone (no. 17 spot), and in the center (no. 18 spot) of aerobic granule used in Co^{2+} adsorption, respectively. Compared to weight % of Co element observed in number 16 (3.11%), 17 (4.26%), and 18 (2.52%) spots, it reveals that Co^{2+} ion uptake has occurred in the whole body of aerobic granule. This result also can explain the phenomena that Co^{2+} adsorption having low affinity in Langmuir model shows high metal uptake value because the whole body can act as an active site for Co^{2+} ion adsorption, even if the affinity for Co uptake is low. Even if the linear plots of $1/Q_e$ against $1/C_e$ show that the adsorption of six different heavy metals ions by aerobic granules fits very well to Langmuir model (Fig. 3), it is not clear that Langmuir model can be recommended to analyze biosorption by granules, because the EDX result showing the whole body of granules can act as an active site for heavy metal sorption which was not corresponded to the Langmuir model's assumption that equilibrium is attained when a monolayer of the adsorbate molecules saturates the adsorbent. It is also verified that there is little difference of the affinity of the adsorbent for the six different ions ($n = 1.23 – 1.52$) in Freundlich model.

As shown in Fig. 7(a)–(c), EDX spectra were observed for Fe^{2+} ions in surface layer (no. 19 spot), in middle zone (no. 20 spot), and in the center

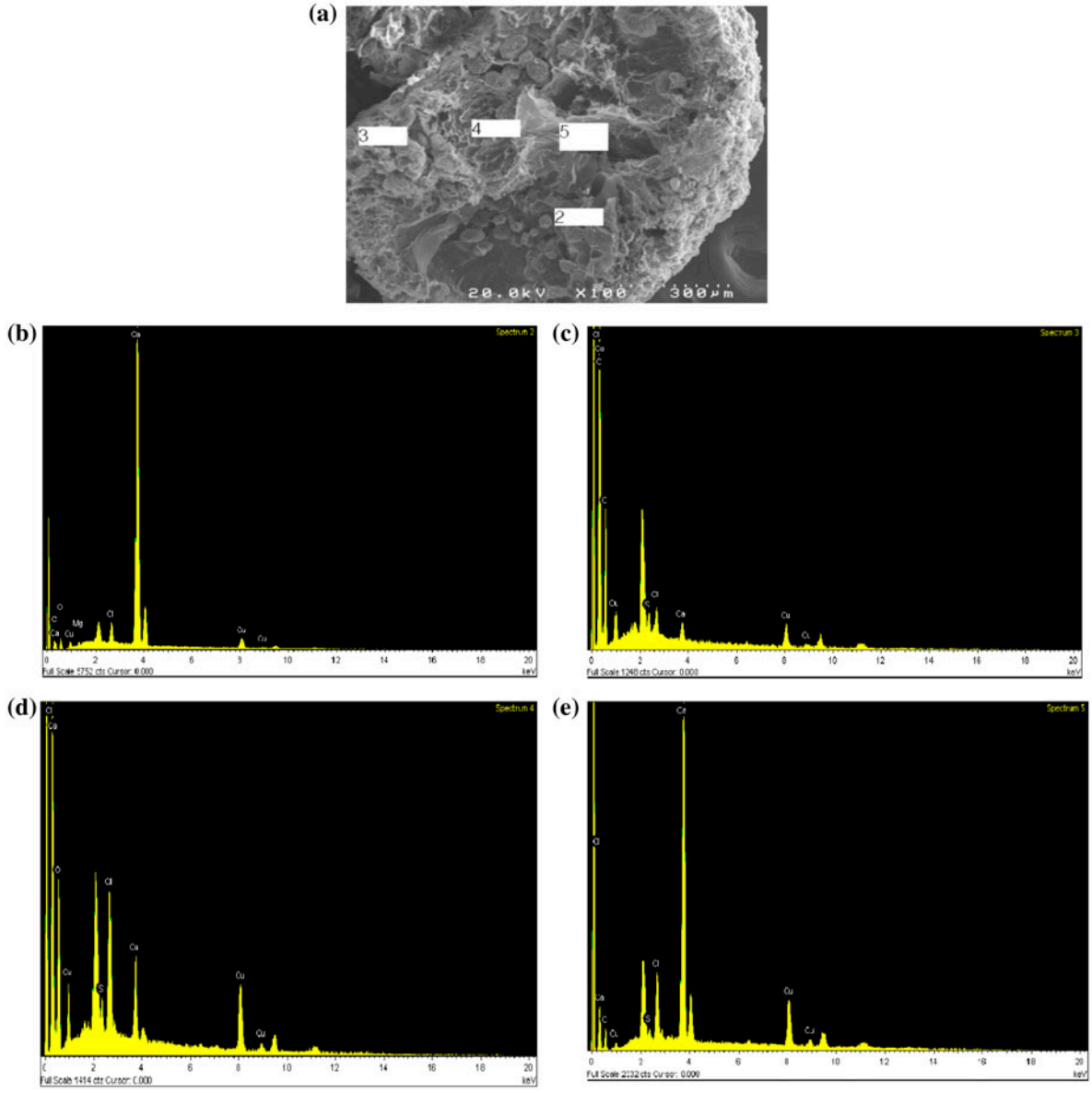

Fig. 5. EDX spectra at specific spots of aerobic granular sludge for Cu^{2+} adsorption [(a): FESEM projection of aerobic granular sludge with scattered spots labeled, (b): EDX spectrum at point 2, (c): EDX spectrum at point 3, (d): EDX spectrum at point 4, and (e): EDX spectrum at point 5].

(no. 21 spot) of aerobic granule used in Fe^{2+} adsorption, respectively, because the highest metal uptake capacity (232 mg of Fe^{2+}/g of granules) was obtained in this experiment. Compared to weight % of Fe element observed in number 19 (21.20%), 20 (24.73%), and 21 (40.78%) spots, it is clear that the penetration of dissolved metal solution to the center of aerobic granule has occurred, which confirms that metal uptake can occur even in the center of aerobic granule. The similar result was also observed in Cu uptake.

The atomic mass percentages of the elements obtained from the EDX analysis are summarized in Table 2. It has been shown that aerobic granules have a porous microbial structure with water channels [40]. Definitely, the porous structure would favor the diffusion of Co^{2+}, Fe^{2+}, and Cu^{2+} to the center of the aerobic granule, as observed in this study. EDX patterns for the other metal case (Cd^{2+}, Mn^{2+}, Zn^{2+}) also showed the similar result (data not shown). The distribution pattern of the adsorbed Ni^{2+} in the aerobic granule revealed that the binding sites for Ni^{2+}

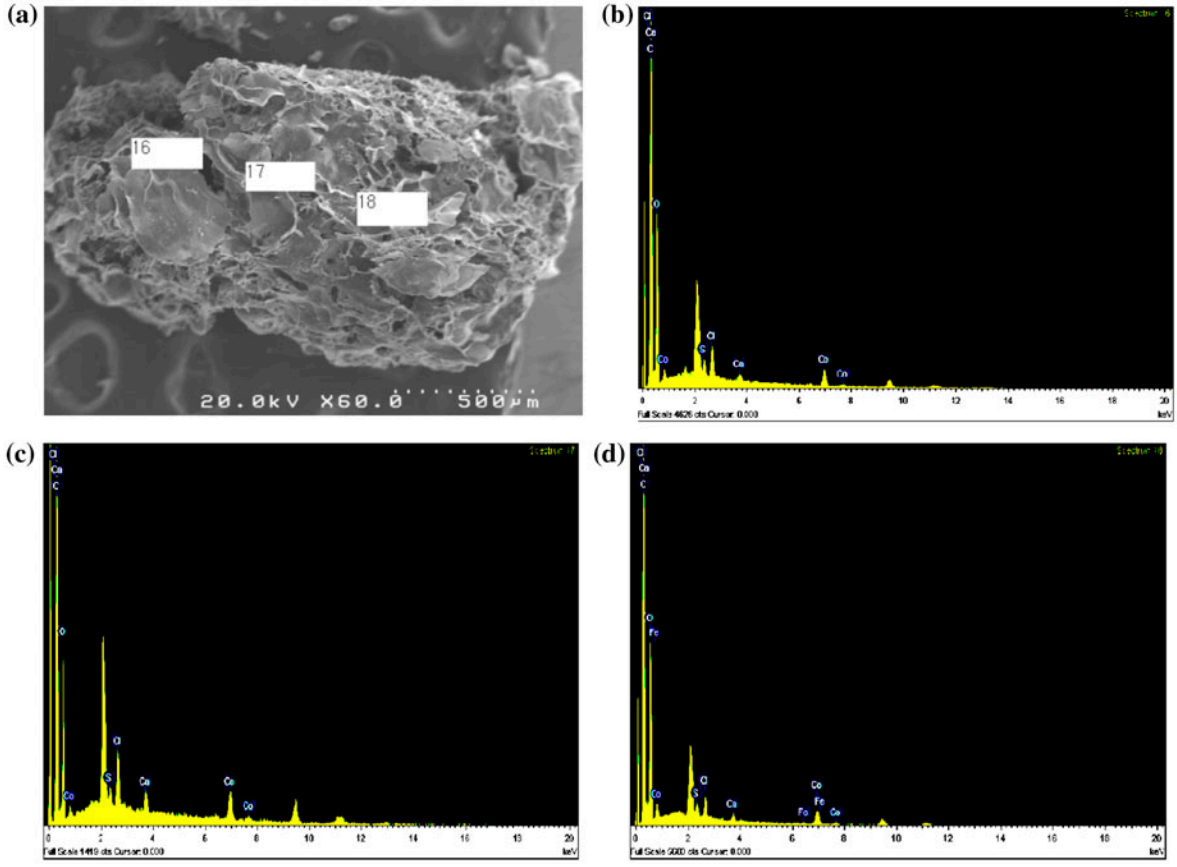

Fig. 6. EDX spectra at specific spots of aerobic granular sludge for Co^{2+} adsorption [(a): FESEM projection of aerobic granular sludge with scattered spots labeled, (b): EDX spectrum at point 16, (c): EDX spectrum at point 17, and (d): EDX spectrum at point 18].

adsorption would be available both on the surface and inside of the aerobic granule [32], in this study, using more various heavy metals, it is verified that the whole body of aerobic granule acted as an active site for metal uptake.

3.4. Contribution of granule functional groups to metal biosorption

3.4.1. Evidence from FTIR analysis

The FTIR spectra of aerobic granules before and after heavy metals biosorption are shown in Fig. 8. These spectra were obtained from scanning in the range of 500–4,000 cm^{-1}. Table 3 lists the main functional groups corresponding to the peaks observed on IR spectra of fresh aerobic granules. The band at 3,274 cm^{-1} represented O–H stretching of polymeric compounds in fresh aerobic granule, and the band at 2,933 cm^{-1} would be due to an asymmetric vibration of CH_2. The bands at 1,735 and 1,382 cm^{-1} could be attributed to the stretching vibration and deformation vibration of C=O of carboxylic acids, respectively. A 1,632 cm^{-1} band was the result of the stretching vibration of C=O and C–N(amide I) peptide bond of protein, while a 1,545 cm^{-1} band would show stretching vibration of C–N and deformation vibration of N–H (amide II) peptide bond of protein. The bands at 1,183 and 1,050 cm^{-1} could be attributed to stretching of C–O–C and OH of polysaccharides, respectively. Some bands observed in the "fingerprint" zone could be attributed to the phosphate or sulphur groups. Compare to Hui and Yu [29], the band, at 2,852 cm^{-1}, that resulted from a symmetric vibration of CH_2 was not observed in fresh aerobic granule in this study.

It appears from Fig. 8 that different functional groups would be responsible for the biosorption of heavy metals. After the biosorption of heavy metals, the broad stretching absorption band at 3,274 cm^{-1} shifted to bands in the range of 3,262–3,290 cm^{-1}, which indicated that amino and hydroxyl groups were

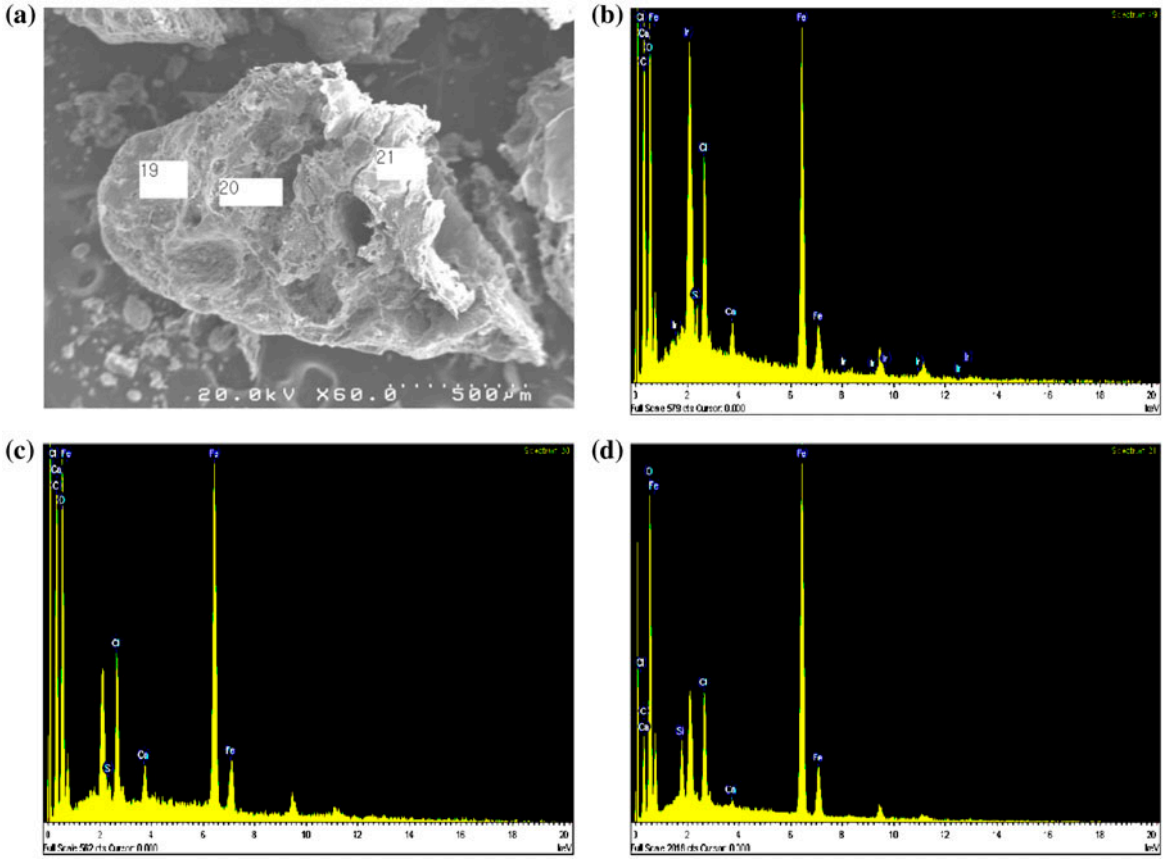

Fig. 7. EDX spectra at specific spots of aerobic granular sludge for Fe^{2+} adsorption [(a): FESEM projection of aerobic granular sludge with scattered spots labeled, (b): EDX spectrum at point 19, (c): EDX spectrum at point 20, and (d): EDX spectrum at point 21].

Table 2
Elemental analyses of the heavy metal adsorbed aerobic granule at different depths from the granule surface

Heavy metals	Major element	Surface zone depth (0–100 μm)		Middle zone depth (100–300 μm)		Center zone depth (300–500 μm)	
		weight %	atomic %	weight %	atomic %	weight %	atomic %
Cu	C	55.87	66.22	–	–	–	–
	O	35.12	31.25	47.07	72.86	19.16	40.24
	Ca	0.97	0.34	8.15	5.04	43.43	36.40
	Cu	6.06	1.36	30.34	11.83	29.16	15.42
Co	C	55.52	64.35	55.48	65.29	54.07	62.68
	O	39.06	33.99	36.41	32.17	41.27	35.91
	Ca	0.36	0.12	1.01	0.36	0.40	0.14
	Co	3.11	0.74	4.26	1.02	2.52	0.60
Fe	C	39.63	57.69	39.34	56.28	20.50	36.57
	O	30.11	32.90	31.78	34.13	32.77	43.90
	Ca	0.68	0.30	0.85	0.37	0.27	0.14
	Fe	21.20	6.64	24.73	7.61	40.78	15.65

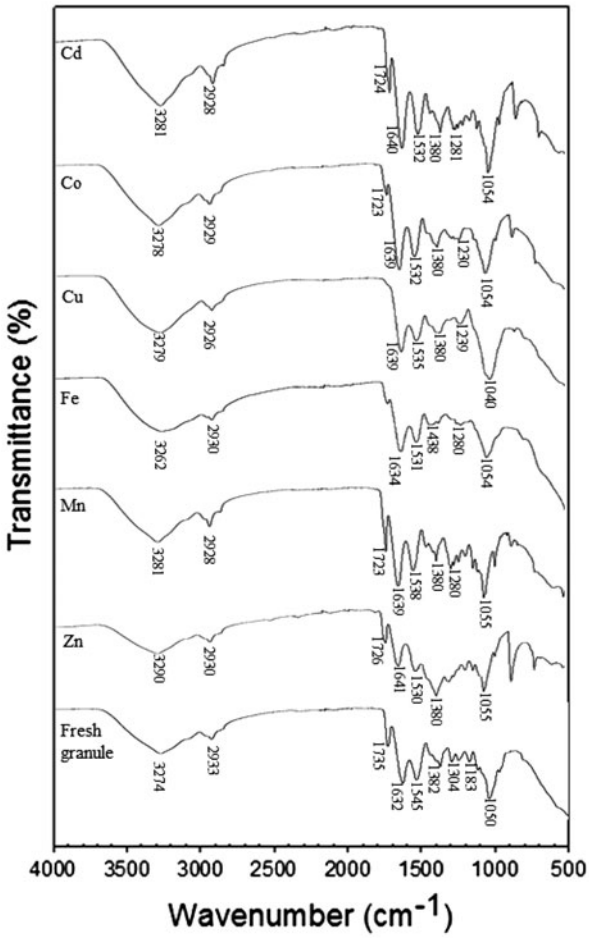

Fig. 8. FTIR spectra of aerobic granules before and after Cd^{2+}, Co^{2+}, Cu^{2+}, Fe^{2+}, Mn^{2+}, and Zn^{2+} biosorption.

responsible for the heavy metal biosorption with aerobic granules, respectively. It is difficult to distinguish which group causes the shift. However, it was observed that the bands shifted to a higher wave number, except Fe^{2+} sorption. After biosorption of Cu^{2+} and Fe^{2+}, the band at 1,735 cm^{-1} disappeared. Meanwhile, after biosorption of Cd^{2+}, Co^{2+}, Mn^{2+}, and Zn^{2+}, the band at 1,735 cm^{-1} shifted slightly to a lower wave number. These results suggest that the carboxyl groups are involved in the binding of heavy metals, i.e. there would be an interaction of heavy metals with carboxyl groups [29,30]. There was no significant shift of the band at 1,632 cm^{-1}, ascribed to the amide I band from proteins. Meanwhile, the peak at 1,545 cm^{-1} of fresh granules, corresponded to the amide II band from proteins, shifted to lower wave numbers, revealing the complexation of heavy metals with the functional groups from proteins.

3.4.2. Evidence from XPS analysis

The XPS survey scanning spectra of aerobic granules before and after Cu^{2+}, Co^{2+}, and Fe^{2+} biosorption are shown in Fig. 9. The elemental peaks detected in the spectrum of fresh aerobic granules are C 1s, N 1s, O 1s, Ca 2s, Ca 2p3, Ca 2p1, and Na 1s, while the peaks of Cu, Fe, and Co were not presented in the XPS survey scanning spectrum of fresh aerobic granules (Fig. 9(a)). The peaks of Co 2p1, Co 2p3, and Co 3s appeared after Co^{2+} biosorption (Fig. 9(b)) and the peaks of Fe 2p1, Fe 2p3, Fe 3s, and Fe 3p appeared after Fe^{2+} biosorption (Fig. 9(c)), respectively. Meanwhile, Cu 2s, Cu 3s, Cu 2p1, Cu 2p3, and Cu 3p

Table 3
Main functional groups on fresh aerobic granule detected by the FTIR

Wave number	Vibration type	Functional type	Wave number [29]
3,274	Overlapping of stretching vibration of OH and NH	OH into polymeric compounds and amine	3,200–3,600
2,933	Asymmetric stretching vibration of CH_2		2,928
1,735	Stretching vibration of C=O	Carboxylic acids	1,725
1,632	Stretching vibration of C=O and C–N (amide I)	Protein (peptide bond)	1,648
1,545	Stretching vibration of C–N and deformation vibration of N–H (amide II)	Protein (peptide bond)	1,520
1,382	Stretching vibration of C=O	Carboxylic acids	
1,183	Stretching vibration of C–O-C	Polysaccharides	1,130–1,160
1,050	Stretching vibration of OH	Polysaccharides	1,056
<1,000	"Fingerprint" zone	Phosphate or sulphur functional groups	<1,000

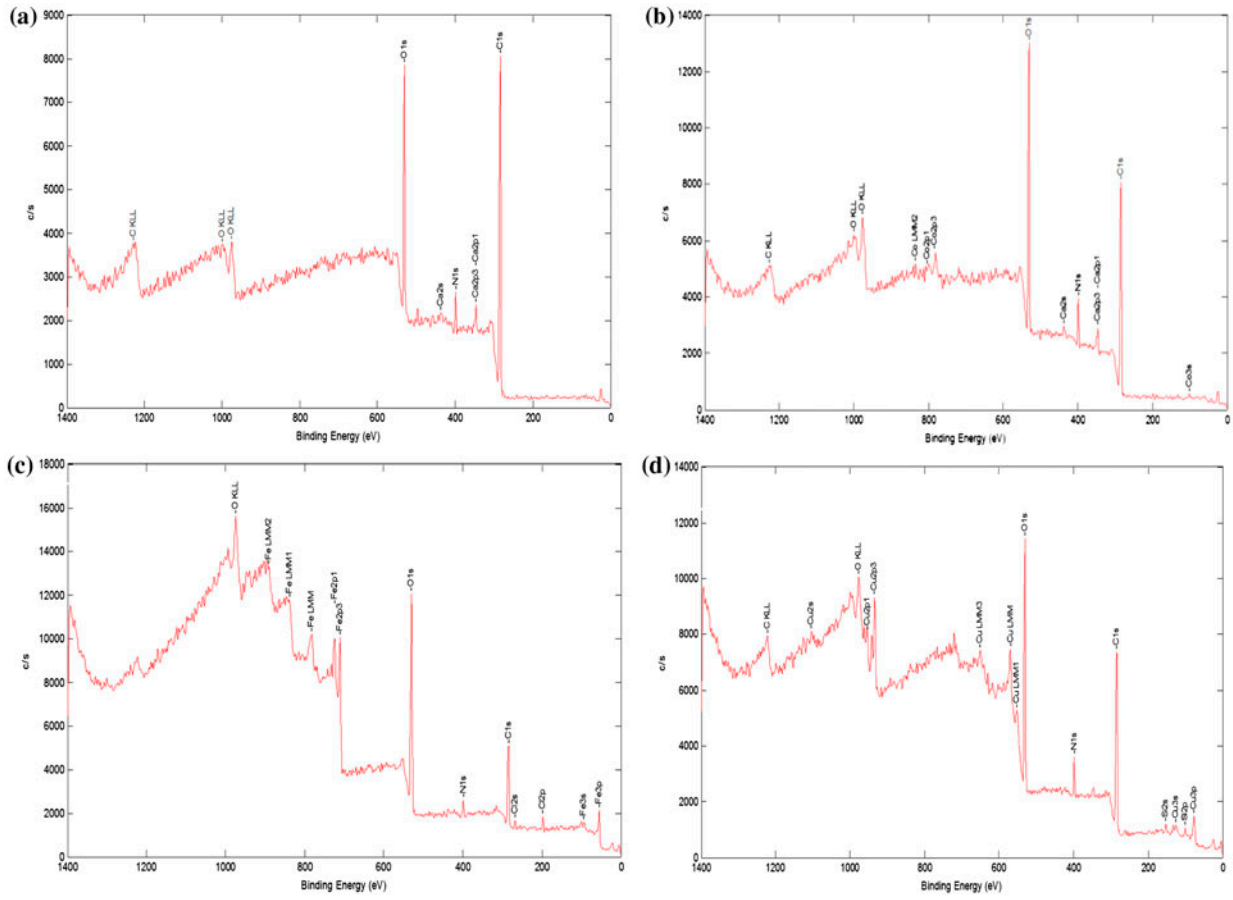

Fig. 9. XPS survey scanning spectrum of aerobic granules before (a) and after Co^{2+} (b), Fe^{2+} (c), and Cu^{2+} (d) biosorption.

appeared in the wide scanning spectrum of aerobic granules after Cu^{2+} biosorption, which demonstrated that Cu was really biosorbed on aerobic granules (Fig. 9(d)). These provide direct evidence that Co, Fe, and Cu can be adsorbed by aerobic granules.

The X-ray photoelectron spectroscopy was used to obtain the elemental information of aerobic granules as well as to illustrate the interaction between the organic functional groups in aerobic granules and the metals adsorbed.

The functional groups were characterized by the BE of C 1s, while the metal ions adsorbed on these functional groups were also analyzed. The changes of BE of the coordination carbon atom (C 1s) in aerobic granules before and after metal biosorption are shown in Fig. 10(a)–(d), and their area ratios are summarized in Table 4. The C 1s spectra of these samples comprise four peaks with corresponding BE of 284.6, 286.0, 288.0, and 289.0 eV that were identified via the deconvolution.

Following to the guidelines for XPS analysis, these peaks are assigned to ether, alcoholic, carboxylate, and carbonate groups, respectively [41]. As shown in Table 4, the area distributions show that the dominant carbon forms in aerobic granules would be ether and alcoholic, respectively. The decrease of ether carbon ratio after metal biosorption (Table 4) indicates that ether-metal species might be formed in aerobic granules. Meanwhile, the area ratios of alcoholic and carboxylate group carbon were also changed, that is, the alcoholic group ratio increased more after Co^{2+} biosorption and the carboxylate group ratio increased after Cu^{2+}, Co^{2+}, and Fe^{2+} biosorption, respectively. There was significant difference between the area ratios before and after Co^{2+} biosorption, but, the carbonate carbon BE peak was not detected after Fe^{2+} biosorption. These seem to indicate that the interaction and coordination affinity between the functional groups and metals would be more complicated than expected [29].

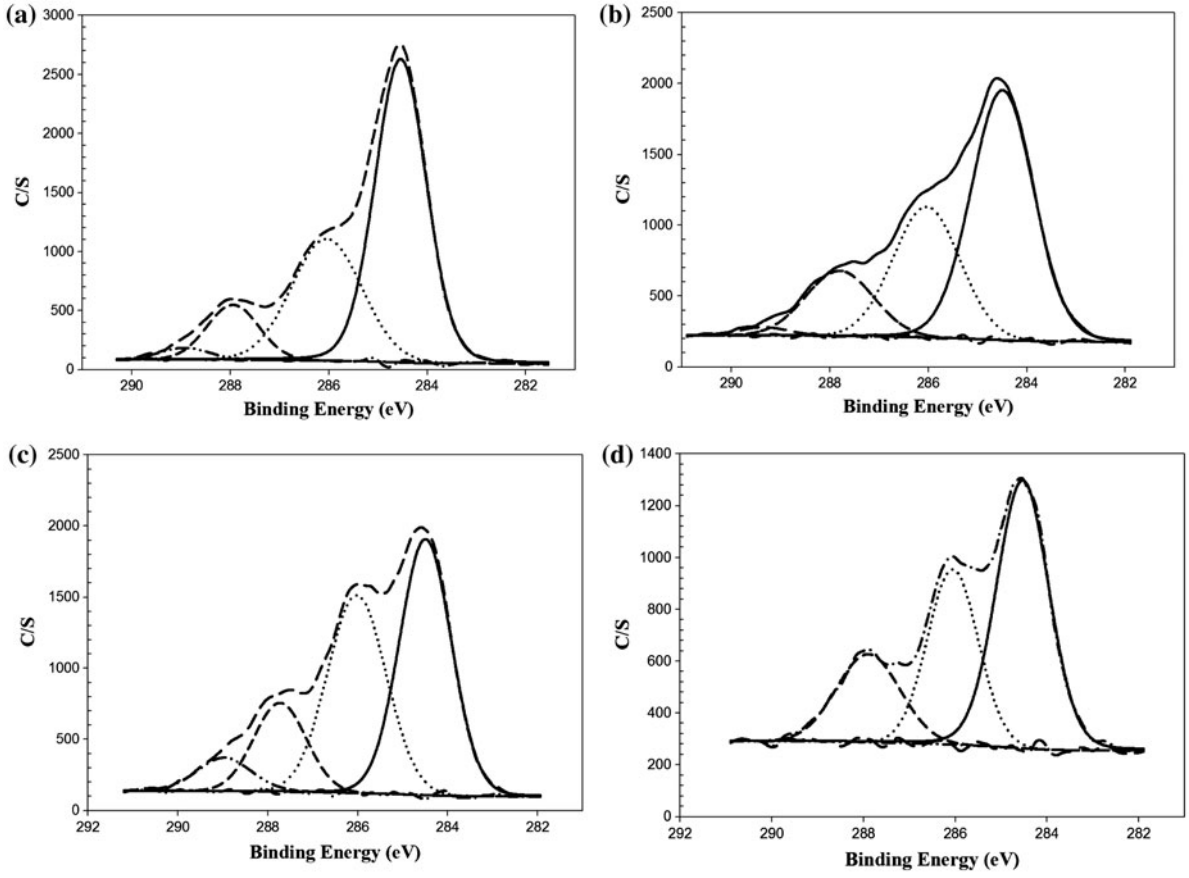

Fig. 10. XPS spectra (C 1s) of aerobic granules before (a) and after Co^{2+} (b), Fe^{2+} (c), and Cu^{2+} (d) biosorption.

Table 4
Summary of binding energies and peak ratios of C 1s spectra before and after heavy metals biosorption

Peak (eV)	Peak area ratio			
	Fresh AG	Cu^{2+}-AG	Fe^{2+}-AG	Co^{2+}-AG
284.6	57.5	54.2	50.2	42.7
286.0	30.4	29.4	30.6	36.7
288.0	10.1	14.9	19.2	14.6
289.0	1.99	1.5	ND	6.0

AG, Aerobic granules; ND, not detected.

4. Conclusions

Aerobic granules showed high capacity of metal adsorption. The analysis of the experimental results of Cd^{2+}, Cu^{2+}, Mn^{2+}, Zn^{2+}, and Co^{2+} biosorption at the same equilibrium pH (6.0) showed that adsorbent affinity followed the order: Cd > Mn > Zn > Cu > Co. Compared with activated sludge [Q_e (mg/g) = 30 – 90] for Cd^{2+} and Cu^{2+} [14], the aerobic granules showed higher adsorption efficiency [Q_e (mg/g) = 189 – 215.4]. For the case of Fe^{2+}, the highest metal uptake capacity was shown as 232 mg of Fe^{2+}/g of granules in the range of pH 2.4–3.4. It was found that both Langmuir and Freundlich isotherm fit the adsorption data well. Especially the R^2 values were larger than 0.96 in most cases when Langmuir model is adopted. In order to look into the distribution of the adsorbed heavy metal in aerobic granules and to verify metal uptake in surface layer, in middle zone, and center of aerobic granule, EDX spectra were obtained.

Based on FESEM-EDX spectra results, it was found that whole granule body including the center can act as an active site for metal uptake because a lot of pore existed inside the aerobic granule. It is clear that the penetration of dissolved metal solution to the center of aerobic granule has occurred, which confirms that metal uptake can occur even in the center of aerobic granule.

The analyses by FTIR and XPS showed that functional groups on aerobic granules, such as alcoholic, carboxylate, and ether, would be the main binding

sites for biosorption of heavy metals. Factors (temperature, pH, EPS content of aerobic granular sludge) affecting the adsorption capacity, competition of heavy metals for adsorption on aerobic granules, and regeneration ability of aerobic granules will be the subject of further investigations.

Acknowledgments

This research was carried out during the first author's internship program in KIST for high school student held on 2011 and research training in the laboratory of Dr Seok Won Hong in KIST during summer vacation on 2012, and was financially supported by the KIST Institutional Program (2E23943). The first author Ki Hong Ahn is extremely grateful to Dr Seok Won Hong for the mentor and co-worker of this research, So Hee Kim in KIST for supporting the analysis of heavy metal ions using ICP-AES & FESEM-EDX, Ji-Eun Kim in KIST for the measurement and data analysis of FTIR, and Hee-Kyoung Kang in KIST for the XPS measurement and data analysis, respectively.

References

[1] A. Hammaini, F. González, A. Ballester, M.L. Blázquez, J.A. Muñoz, Biosorption of heavy metals by activated sludge and their desorption characteristics, J. Environ. Manage. 84 (2007) 419–426.
[2] A. Esposito, F. Pagnanelli, A. Lodi, C. Solisio, F. Vegliò, Biosorption of heavy metals by *Sphaerotilus natans*: an equilibrium study at different pH and biomass concentrations, Hydrometallurgy 60 (2001) 129–141.
[3] B. Yuncu, F.D. Sanin, U.J. Yetis, An investigation of heavy metal biosorption in relation to C/N ratio of activated sludge, J. Hazard. Mater. 137 (2006) 990–997.
[4] F. Pagnanelli, M. Trifoni, F. Beolchini, A. Esposito, L. Toro, F. Vegliò, Equilibrium biosorption studies in single and multi-metal systems, Process Biochem. 37 (2001) 115–124.
[5] L. Velásquez, J.J. Dussan, Biosorption and bioaccumulation of heavy metals on dead and living biomass of *Bacillus sphaericus*, J. Hazard. Mater. 167 (2009) 713–716.
[6] B. Volesky, Biosorption and me, Water Res. 41 (2007) 4017–4029.
[7] R. Say, A. Denizli, M.Y. Arica, Biosorption of cadmium(II), lead(II) and copper(II) with the filamentous fungus *Phanerochaete chrysosporium*, Bioresour. Technol. 76 (2001) 67–70.
[8] S. Senthilkumaar, S. Bharathi, D. Nithyanandhi, V. Subburam, Biosorption of toxic heavy metals from aqueous solutions, Bioresour. Technol. 75 (2000) 163–165.
[9] Y. Sag, T. Kutsal, Determination of the biosorption activation energies of heavy metal ions on *Zoogloea ramigera* and *Rhizopus arrhizus*, Process Biochem. 35 (2000) 801–807.
[10] M.M. Figueira, B. Volesky, V.S.T. Ciminelli, A. Roddick, Biosorption of metals in brown seaweed biomass, Water Res. 34(1) (2000) 196–204.
[11] A.H. Hawari, C.N. Mulligan, Biosorption of lead(II), cadmium(II), copper(II) and Nickel(II) by anaerobic granular biomass, Bioresour. Technol. 97 (2006) 692–700.
[12] P. Dostalek, M. Patzak, P. Matejka, Influence of specific growth limitation on biosorption of heavy metals by *Saccharomyces cerevisiae*, Int. Biodeterior. Biodegrad. 54 (2004) 203–207.
[13] Y.C. Lee, S.P. Chang, The biosorption of heavy metals from aqueous solution by *Spirogyra* and *Cladophora* filamentous macroalgae, Bioresour. Technol. 102 (2011) 5297–5304.
[14] Z. Al-Qodah, Biosorption of heavy metal ions from aqueous solutions by activated sludge, Desalination 196 (2006) 164–176.
[15] W.Y. Baik, J.H. Bae, K.M. Cho, W. Hartmeier, Biosorption of heavy metals using whole mold mycelia and parts thereof, Bioresour. Technol. 81 (2002) 167–170.
[16] Y. Liu, S.F. Yang, H. Xu, K.H. Woon, Y.M. Lin, J.H. Tay, Biosorption kinetics of cadmium(II) on aerobic granular sludge, Bioresour. Technol. 38 (2003) 997–1001.
[17] A.J.M. Barros, S. Prasad, V.D. Leite, A.G. Souza, Biosorption of heavy metals in upflow sludge columns, Bioresour. Technol. 98 (2007) 1418–1425.
[18] F. Pagnanelli, F. Beolchini, A. Esposito, L. Toro, F. Vegliò, Mechanistic modeling of heavy metal biosorption in batch and membrane reactor systems, Hydrometallurgy 71 (2003) 201–208.
[19] W.C. Chang, G.S. Hsu, S.M. Chiang, M.C. Su, Heavy metal removal form aqueous solution by wasted biomass from a combined AS-biofilm process, Bioresour. Technol. 97 (2006) 1503–1508.
[20] S. Sirianuntapiboon, O. Ungkaprasatcha, Removal of Pb^{2+} and Ni^{2+} by bio-sludge in sequencing batch reactor (SBR) and granular activated carbon-SBR (GAC-SBR) systems, Bioresour. Technol. 98 (2007) 2749–2757.
[21] G. Yan, T. Viraraghavan, Heavy metal removal in a biosorption column by immobilized *M. rouxii* biomass, Bioresour. Technol. 78 (2001) 243–249.
[22] G. Bayramoglu, S. Bektas, M.Y. Arica, Biosorption of heavy metal ions on immobilized white-rot fungus Trametes versicolor, J. Hazard. Mater. 101 (2003) 285–300.
[23] H.H. Alaa, N.M. Catherine, Heavy metals uptake mechanisms in a fixed-bed column by calcium—Treated anaerobic biomass, Process Biochem. 41 (2006) 187–198.
[24] S.S. Adav, D.J. Lee, K.Y. Show, J.H. Tay, Aerobic granular sludge: Recent advances, Biotechnol. Adv. 26 (2008) 411–423.
[25] Y. Liu, S.F. Yang, J.H. Tay, Q.S. Liu, L. Qin, Y. Li, Cell hydrophobicity is a triggering force of biogranulation, Enzyme Microb. Technol. 34 (2004) 371–379.
[26] J.J. Beun, A Hendriks, M.C.M van Loosdrecht, E. Morgenroth, P.A. Wilderer, J.J. Heijnen, Aerobic granulation in a sequencing batch reactor, Water Res. 33(10) (1999) 2283–2290.
[27] H. Xu, Y. Liu, J.H. Tay, Effect of pH on nickel biosorption by aerobic granular sludge, Bioresour. Technol. 97 (2006) 359–363.

[28] S. Fang, S. Weiling, S. Haimei, N. Jinren, Biosorption behavior and mechanism of beryllium from aqueous solution by aerobic granule, Chem. Eng. J. 172 (2011) 783–791.
[29] X. Hui, L. Yu, Mechanisms of Cd^{2+}, Cu^{2+} and Ni^{2+} biosorption by aerobic granules, Sep. Purif. Technol. 58 (2008) 400–411.
[30] Y. Lei, Y. Zhengfang, T. Meiping, L. Peng, N. Jinren, Removal of Cr^{3+} from aqueous solution by biosorption with aerobic granules, J. Hazard. Mater. 165 (2009) 250–255.
[31] W. Xinhua, S. Ruihong, T. Shaoxiang, G. Mingming, N. Jianyuan, L. Feifei, W. Shuguang, G. Baoyu, Characteristics and mechanisms of Cu(II) biosorption by disintegrated aerobic granules, J. Hazard. Mater. 179 (2010) 431–437.
[32] L. Yu, X. Hui, Equilibrium, thermodynamics and mechanisms of Ni^{2+} biosorption by aerobic granules, Biochem. Eng. J. 35 (2007) 174–182.
[33] L. Yongqiang, T. Joohwa, Cultivation of aerobic granules in a bubble column and an airlift reactor with divided draft tubes at low aeration rate, Biochem. Eng. J. 34 (2007) 17.
[34] B. Volesky, Removal and recovery of heavy metals by biosorption. in: B. Volesky (Ed.) Biosorption of Heavy Metals. 1st ed. CRC, Boca Raton, 1990, pp. 20–25.
[35] G. Ozdemir, T. Ozturk, N. Ceyhan, R. Isler, T. Cosar, Heavy metal biosorption by biomass of *Ochrobactrum anthropi* producing exopolysaccharide in activated sludge, Bioresour. Technol. 90 (2003) 71–74.
[36] Z. Liu, Z.W. Wang, Essential roles of extracellular polymeric substances in aerobic granulation. in: Y. Liu (Ed.) Aerobic Granulation in Sequencing Batch Reactors. 1st ed. CRC, Boca Raton, 2008, pp. 181–194.
[37] Z.W. Wang, Y. Li, J.Q. Zhou, Y. Liu, The influence of short-term starvation on aerobic granules, Process Biochem. 41 (2006) 2373–2378.
[38] Y. Nuhoglu, E. Oguz, Removal of copper(II) from aqueous solutions by biosorption on the cone biomass of *Thuja orientalis*, Process Biochem. 38 (2003) 1627–1631.
[39] A. Selatnia, A. Madani, M.Z. Bakhti, L. Kertous, Y. Mansouri, R. Yous, Biosorption of Ni^{2+} from aqueous solution by a NAOH-treated bacterial dead *Streptomyces rimosus* biomass, Miner. Eng. 17 (2004) 903–911.
[40] J.H. Tay, V. Ivanov, S. Pan, S.T.L. Tay, Specific layers in aerobically grown microbial granules, Lett. Appl. Microbiol. 34 (2002) 254–257.
[41] P.X. Sheng, Y.P. Ting, J.P. Chen, L. Hong, Sorption of lead, copper, cadmium, zinc, and nickel by marine algal biomass: characterization of biosorptive capacity and investigation of mechanisms, J. Colloid Interface Sci. 275 (2004) 131–141.